Article

Giant Unilamellar Vesicles Formed by Hybrid Films of Agarose and Lipids Display Altered Mechanical Properties

Rafael B. Lira,[1,2] Rumiana Dimova,[2] and Karin A. Riske[1,*]

[1]Departamento de Biofísica, Universidade Federal de São Paulo, São Paulo, Brazil; and [2]Department of Theory and Bio-Systems, Max Planck Institute of Colloids and Interfaces, Potsdam, Germany

ABSTRACT   Giant unilamellar vesicles (GUVs) are presumably the current most popular biomimetic membrane model. Preparation of GUVs in physiological conditions using the classical electroformation method is challenging. To circumvent these difficulties, a new method was recently reported, by which GUVs spontaneously swell from hybrid films of agarose and lipids. However, agarose is left encapsulated in the vesicles in different amounts. In this work, we thoroughly characterize the mechanical properties of these agarose-GUVs in response to electric pulses, which induce vesicle deformation and can lead to membrane poration. We show that the relaxation dynamics of deformed vesicles, both in the presence and absence of poration, is significantly slowed down for agarose-GUVs when compared to agarose-free GUVs. In the presence of poration, agarose polymers prevent complete pore closure and lead to high membrane permeability. A fraction of the vesicles were found to encapsulate agarose in the form of a gel-like meshwork. These vesicles rupture and open up after electroporation and the meshwork is expelled through a macropore. When the agarose-GUVs are heated above the melting temperature of agarose for 2 h before use, vesicle response is (partially) recovered due to substantial release of encapsulated agarose during temperature treatment. Our findings reveal potential artifactual behavior of agarose-GUVs in processes involving morphological changes in the membrane as well as poration.

INTRODUCTION

Biomembranes define the boundaries of all cells, separating the external fluids from the intracellular compartment and allowing controlled exchange of materials. They also impart mechanical stability to the cell, control cellular migration and adhesion, and play a key role in energy conversion. Phenomena involving biological membranes are, however, very complex and intricate, because numerous processes occur interrelated and concurrently, making their study not trivial and easily prone to interferences.

The use of model membranes allows one to modify simply and independently many parameters at a time and to probe the events of interest without interfering contributions from parallel processes occurring in the membranes of living cells. Among all membrane models of biological membranes, giant unilamellar vesicles (GUVs) are presumably one of the best suited and increasingly employed for several reasons. They are closed freestanding lipid bilayers that faithfully mimic the size and curvature of the plasma membrane and can be directly visualized and manipulated under a microscope (1–3). These features make them an ideal system for investigating a variety of membrane properties and membrane-related processes.

Traditionally, GUVs have been used to study biophysical properties of membranes including elasticity (4,5) and

domain formation (6,7), their interaction with membrane active molecules (8) and nanoparticles (9,10), membrane wetting (11), vesicles as chemical reactors (12,13) and artificial cells (14), and for many other applications (15,16). Currently, there is a large variety of methods for production of GUVs (3,15) such as the classical electroformation method (17) (with some recent modifications (18)), simple gentle hydration (19), phase-reverse evaporation (20), emulsion and microfluidic methods (14,21). Although some protocols are very simple, requiring solely the hydration of a lipid stack with a nonionic solution, others require sophisticated equipment, are time-consuming, or lead to contaminations of precursor materials (15,21). Moreover, most of them work only for a restricted range of lipid compositions and usually do not allow vesicle production in ionic buffered solutions.

Recently, Horger et al. (22) reported a simple and very robust method to prepare GUVs in solutions of high ionic strength using virtually any membrane composition. The method relies on hydrating a film of lipids deposited on a preformed film of agarose, yielding vesicles in a few minutes in a simple and straightforward way. This method represents a very important step in the development of protocols for preparation of GUVs and has been the method of choice for producing GUVs in a number of studies (23–28). However, agarose is left as a residual contamination in the formed vesicles, even though it has been reported not to change the molecular mobility of lipids in the bilayer (22). Given the significance of the method, we considered it important to

CrossMark

evaluate how the residual polymer affects the overall membrane mechanics rather than simply the lipid diffusion. A subsequent work replaced agarose with the chemically cross-linked polyvinyl alcohol (PVA) to circumvent polymer encapsulation (29). However, the difficulty in detaching the formed GUVs from the PVA film is still an issue.

Here, we studied the effects of residual agarose on the mechanical properties of GUVs grown from hybrid films of agarose and lipids. To assess the mechanical properties of GUVs, we made use of vesicle response to electric pulses, which are able to deform the vesicles and lead to poration of the membrane (30–33). After the end of the pulse, the vesicles relax back to their original shape and pores would typically reseal, restoring the membrane integrity. The dynamics of these processes are governed by material properties of the lipid bilayer such as edge tension, bending rigidity, and membrane viscosity (30–32,34). We investigated the effects of residual agarose on i), membrane permeability; ii), vesicle relaxation after the application of an electric pulse; and iii), pore lifetime in porated vesicles. The results obtained with GUVs grown in hybrid films of agarose/lipid are compared to those of polymer-free GUVs prepared with the conventional electroformation method. We show that the presence of agarose residues hinders the mechanical response of GUVs and increases membrane permeability. Our findings have implications to studies on membrane dynamics and morphological changes as well as poration of such vesicles.

MATERIALS AND METHODS

Materials

The phospholipids 1-palmitoyl-2-oleoyl-*sn*-glycero-3-phosphocholine (POPC) and 1-palmitoyl-2-oleoyl-*sn*-glycero-3-phospho-(1′-rac-glycerol), sodium salt (POPG), and the fluorescent probes 1,2-dipalmitoyl-*sn*-glycero-3-phosphoethanolamine-*N*-(7-nitro-2-1,3-benzoxadiazol-4-yl) (DPPE-NBD) and 1,2-dipalmitoyl-*sn*-glycero-3-phosphoethanolamine-*N*-(lissamine rhodamine B sulfonyl) (DPPE-Rh) were purchased from Avanti Polar Lipids (Alabaster, AL). Sulforhodamine B, Fluorescein isothiocyanate isomer I (FITC), ultralow gelling temperature type IX-A agarose, sucrose, glucose, and NaCl were purchased from Sigma Aldrich (St. Louis, MO). Low gelling temperature agarose was purchased from Fisher Scientific (Waltham, MA). All chemicals were used without further purification. Milli-Q water was used throughout the work.

GUV preparation

GUVs were prepared either by the classical electroformation method (17) or by hydration of hybrid films of agarose and lipids (22). Two different membrane compositions were used: neutral membranes made of pure POPC and charged membranes made of POPC/POPG 8:2 (molar ratio). When needed, 0.5 mol % of either DPPE-NBD or DPPE-Rh were added to the lipid solution. For electroformation, 8–10 μL of a 3 mM lipid solution in chloroform were spread on a pair of conductive glasses coated with indium tin oxide. Solvent was evaporated by a stream of N_2 for 5 min (note that evaporation under vacuum for 2 h did not lead to a difference in the vesicle behavior). The glasses were sandwiched using a 1 mm Teflon spacer forming a chamber with ~1.5 mL volume and coupled to a function generator. AC field of 1 V at

10 Hz was applied and 0.2 M sucrose solution was added to the chamber. Vesicles were allowed to grow for 1 h at room temperature.

Growing GUVs from hybrid films of agarose and lipids was performed as in Horger et al. (22) with minor modifications. A 1% (w/v) agarose solution was prepared in pure water above the polymer melting temperature T_m and stored at 4°C. Before use, the solution was heated above T_m and ~200 μL were spread over a clean coverglass placed on a heating plate at 80°C for ~15 min to ensure evaporation of excess water. 8–10 μL of a 3 mM of the lipid solution in chloroform were then spread over this agarose film and dried with a stream of N_2. A chamber was assembled with a Teflon spacer and filled with sucrose solution as previously mentioned. Vesicles were allowed to grow for 30 min at room temperature.

In some experiments, fluorescently labeled agarose was also used. Labeling with FITC was performed as in Horger et al. (22) for low and ultralow gelling temperature agarose. Labeled agarose was then diluted 10 times in the respective nonlabeled solution and stored at 4°C before use. In some experiments, 2.5 μM sulforhodamine B was added to the sucrose solution used to grow GUVs. When fluorescent dyes were used, swelling was carried out in the dark.

Vesicles were dispersed in isoosmolar glucose solution. The osmolarities of sucrose and glucose solutions were carefully adjusted using cryoscopic osmometer Osmomat 030 (Gonotec, Berlin, Germany).

Microscopy observation and image analysis

Different microscope setups were used depending on the type of experiment. Usually, a Zeiss Axiovert 200 (Jena, Germany) phase contrast microscope was used for GUV observation and quantification of vesicle relaxation and pore lifetime after pulse application. For statistical counting, a 10× objective (NA 0.25) was used to record a larger number of GUVs. For recording a typical event, a 40× or 63× air objective (NA 0.6 and 0.75, respectively) was used. The microscope was equipped with a Zeiss Axio-Cam HSm camera and movies were recorded at 60 frames per second during pulse application. Alternatively, fast fluorescence recording was performed at 5 ms temporal resolution using a Zeiss Axio Observer.D1 microscope equipped with a sCMOS camera (pco.edge, PCO AG, Kelheim, Germany). Vesicles were observed either with a 20× (NA 0.5) or a 40× (NA 0.6) objective. In the same setup, phase contrast images were also recorded. For high temporal resolution recordings under phase contrast, a fast digital camera HG-100 K (Redlake, San Diego, CA) was used at an acquisition speed of 10,000 frames per second. Sample illumination was achieved with a mercury lamp HBO W/2.

Confocal microscopy was used to quantify the amount of agarose inside vesicles and release of encapsulated materials after pulse application. Vesicle observation was done under a confocal microscope (Leica TCS SP5, Wetzlar, Germany) through a 40× (0.75 NA) air or 63× (1.2 NA) water immersion objectives. DPPE-NBD and FITC-labeled agarose were excited with an argon laser at 488 nm and sulforhodamine B and DPPE-Rh were excited with a diode-pumped solid-state laser at 561 nm. The emission signals were collected at 500–555 nm and 565–620 nm bands, respectively. To record vesicle deformation and poration, images were acquired at 15 ms time resolution.

The amount of fluorescence of agarose inside the vesicles was quantified using ImageJ (NIH, USA) as a density of agarose fluorescence (average fluorescence intensity over a defined circular area). Identical settings of the confocal microscope were applied for acquiring all images. Vesicle deformation was analyzed by manually measuring GUV dimensions using a Zeiss AxioVision software or by an in-house software for detecting membrane contours as described elsewhere (35).

Pulse application

Direct current (DC) pulses were applied using an Eppendorf multiporator (Eppendorf, Germany), in which field strength and duration can be

controlled from 50 to 300 V and 50 to 300 μs, respectively. This porator was used in most experiments described here. A single pulse of 150 V/150 μs duration was applied for all cases when not mentioned otherwise. Alternatively, a pulse generator GHT_Bi500 (βtech l'Union, Saint-Orens-de-Gameville, France) synchronized with the fast digital camera was used for vesicle deformation (30 V/600 μs). The pulses were applied to vesicles placed in a modified electrofusion chamber (Eppendorf) with parallel cylindrical electrodes (92 μm radius) spaced at 500 μm (36).

RESULTS

Agarose is a polymer consisting of polysaccharide chains of varying length (22,37). It is known to exhibit significant hysteresis in the gel-to-liquid transition, with a notable difference between the melting, T_m, and gelling, T_g, temperatures (37). Here, we use two different types of agarose, low and ultralow gelling temperature agarose, for which, T_m ~58°C and 52°C, and T_g ~26°C and 18°C, respectively. Agarose fluorescently labeled with FITC was also prepared to allow observations with fluorescence microscopy. No difference in the GUV response was observed depending on the agarose type. We present the data obtained with GUVs grown with low gelling temperature agarose, termed here agarose-GUVs. Results obtained with GUVs prepared with ultralow gelling temperature agarose are shown in the Supporting Material. For comparison, the mechanical response of GUVs formed by the classical electroformation method in the absence of agarose, termed as agarose-free GUVs, was also studied. We grew the vesicles in sucrose solution and dispersed them in isoosmolar glucose solution, thus enhancing the optical contrast of GUVs and facilitating the detection of the vesicle contour and macropores in phase contrast images. We chose to work mainly in salt-free media because of the limitations of our method to evaluate the mechanical response of the vesicles: application of strong DC pulses to solutions with high ionic strength leads to sample heating, shorter charging time of the membrane, and nonspherical vesicle deformation (32), complicates the analysis. We explored both neutral membranes made of pure POPC and charged ones made of POPC/POPG 8:2 (molar ratio). The latter composition was investigated in more detail, as this is the typical composition of GUVs grown by the simple gentle hydration method (19). Both charged and neutral GUVs exhibited similar behavior. Here, we present data with the charged membranes. A direct comparison between charged and neutral GUVs is shown in the Supporting Material and will be discussed ahead.

Agarose-GUVs prepared in films of fluorescent agarose display homogeneous fluorescence in their aqueous lumen (Fig. S1 A). In salt-free media as used here, agarose is only left encapsulated in the vesicle lumen without significant binding to membranes (Fig. S1 A). However, when 100 mM NaCl was present in both the growing and the dispersing media (mimicking the conditions used in the original work of Horger et al. (22)), polymer fluorescence

was observed in the vesicle lumen and at the vesicle surface (Fig. S1 B). In the conditions tested here, where no salt is present, lipid mobility was not affected by the encapsulated polymer (compared to agarose-free GUVs), as probed by fluorescence recovery after photobleaching (Fig. S2), confirming previous findings (22). Some fraction of the agarose-GUVs in the sample (~10–20%) presented a visibly higher concentration of encapsulated agarose, as judged from the high intensity of encapsulated fluorescent agarose and from phase contrast images, which showed the presence of a meshwork inside such vesicles. These vesicles appeared stiff, with no visible membrane fluctuations and at times with nonspherical shapes, suggesting that the encapsulated polymer was in a gel-like state. Several examples of such stiff agarose-GUVs are shown in Fig. S3. It is evident that vesicles with such stiff meshwork inside exhibit altered overall mechanical properties.

Encapsulated agarose is in its gel state at room temperature. To investigate whether melting of agarose has an effect on its encapsulation in vesicles, agarose-GUVs grown (at room temperature) with fluorescent agarose were heated at 70°C for 2 h and then allowed to cool down to room temperature. Such temperature-treated GUVs will be termed heated agarose-GUVs in the following. Fluorescence intensity of the encapsulated agarose was measured from confocal microscopy images as the average intensity inside the vesicles. Images in Fig. 1 show typical agarose fluorescence before and after temperature treatment and the graph below displays fluorescence intensity measured for many vesicles before and after temperature treatment. Agarose-GUVs without temperature treatment exhibit a large variation in the amount of encapsulated agarose (Fig. 1). After heating, fluorescence inside the vesicles is reduced around fourfold, indicating that agarose-GUVs become permeable during temperature treatment, allowing the escape of a significant amount of the encapsulated agarose. To probe whether this high membrane permeability at 70°C was specific to agarose-GUVs only, we imposed sugar asymmetry across the membrane of both agarose-GUVs and agarose-free GUVs before temperature treatment. When observed under phase contrast after cooling to room temperature, only the agarose-GUVs had lost their sugar asymmetry, whereas agarose-free GUVs retained their original contrast (not shown).

Mechanical responses of agarose-GUVs were assessed from their response to electric pulses. Strong DC pulses deform vesicles, ultimately leading to membrane electroporation when the so-called lysis tension is reached (30,31). After the end of the pulse, the vesicle relaxes back to its original shape and the formed pores typically reseal driven by the membrane edge tension (34). In a previous work, it was shown that the relaxation dynamics of GUVs made of egg-PC is characterized by up to three characteristic times depending on the vesicle and the pulse conditions (31): a fast relaxation time τ_1 (~0.1 ms) resulting from the
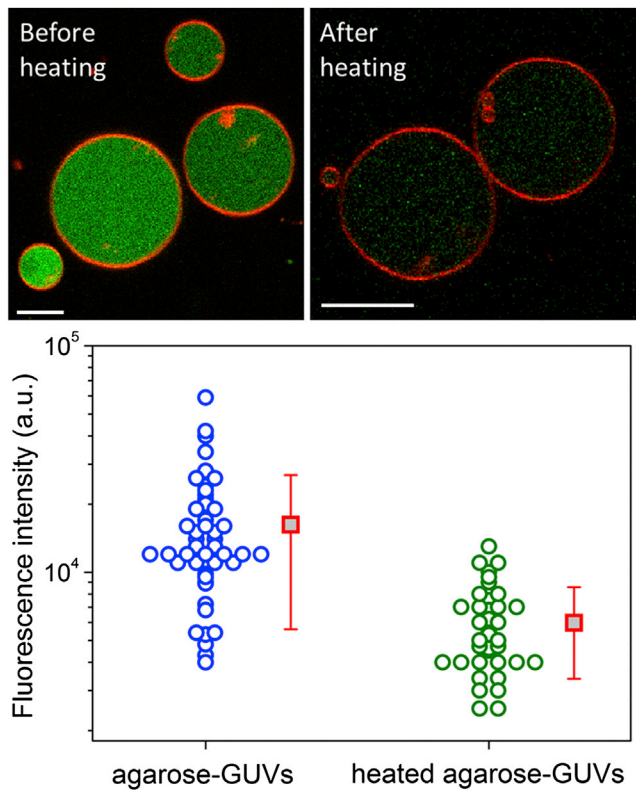
FIGURE 1 Thermal treatment of preformed agarose-GUVs releases polymer from vesicle interior. Images show agarose-GUVs made in films of fluorescent agarose, before (*left*) and after (*right*) temperature treatment. Bars: 10 μm. The membrane is labeled with 0.5 mol % DPPE-Rh. Below, agarose fluorescence inside vesicles before (*blue*) and after (*green*) heating. Red squares show mean values with standard deviation. To see this figure in color, go online.

relaxation of acquired membrane tension in nonporated GUVs, an intermediate time τ_2 (~10 ms) related to pore closure, and a much slower relaxation time τ_3 (~1 s) due to fluid displacement in vesicles with excess area.

Single DC pulses (of field strength 3 kV.cm^{-1} and duration 150 μs, when not otherwise mentioned) were used to deform and porate agarose-free, agarose-, and heated agarose-GUVs. In these conditions, all analyzed GUVs (typically with diameter larger than 20 μm) porate, regardless of their initial tension. As reported previously (31), application of DC pulses of similar magnitude to bare egg-PC GUVs in the absence of salt causes prolate deformation and opening of macropores of a few micrometers in size. Under phase contrast observations, macropores can be visualized as the leakage of the inner sucrose solution through the formed macropores. The halo around the vesicle surface is disrupted by spikes of sucrose solution leaking through the pores. After the pulse, the vesicle relaxes to its original spherical shape and the macropores reseal, restoring the original halo (31). In sharp contrast, application of such electric pulses to agarose-GUVs leads to unusual responses.

Some agarose-GUVs, mainly those encapsulating a considerably high concentration of agarose in the form of a gel-like meshwork (see Fig. S3), ruptured in response to pulse application and the meshwork was pushed out. Below we will refer to this process as rupture with expulsion. One such example is shown in the upper row of images in Fig. 2 *A* and Movie S1. Note that these vesicles appear to be also very stiff, and the application of the pulse causes only a very small and short-lived (<0.2 ms) prolate deformation (data not shown). The lower row of images in Fig. 2 *A* shows the rupture sequence of another vesicle observed with confocal microscopy. A very large pore opens (follow the *green fluorescence* from the membrane probe in Fig. 2 *A*) leading to a fast and complete escape of the encapsulated dye (*red*). The large pore eventually closes and the membrane recloses into a smaller vesicle (see vesicle indicated with an *arrowhead* in the last snapshot of Fig. 2 *A*, >10 s. The vesicle diameter is reduced by ~15%).

Interestingly, for most of the remaining GUVs, which did not exhibit rupture and expulsion upon pulse application but underwent normal pore closure, increased membrane permeability was detected after the pulse. This permeable state was detected either by loss of optical contrast under phase contrast—upper row in Fig. 2 *B*, or by leakage of the encapsulated fluorescent probe—lower row in Fig. 2 *B* and Movie 2. These processes occurred on a slow timescale (seconds to minute) indicating the presence of persisting submicron pores in apparently intact GUVs, allowing the passage of sugars and fluorescent probes across the membrane. The vesicles, which underwent rupture and expulsion followed by reclosing, presumably also exhibit high membrane permeability but because the event is so drastic, the sugar and fluorescence contrast is lost already during the expulsion.

Both phenomena of vesicle rupture-expulsion and long-lasting permeable state were observed very frequently after pulse application. To estimate the frequency of occurrence of both phenomena, the fraction of GUVs exhibiting vesicle rupture and expulsion, $X_{rupture}$, and postpulse leaky state, X_{leak}, was measured for a large number of vesicles observed in phase contrast mode. The results are shown in Fig. 2 *C*. For agarose-free GUVs, virtually no vesicle rupture or permeable vesicles were observed. In sharp contrast, a large number of agarose-GUVs exhibited rupture, $X_{rupture} = 0.2 \pm 0.1$, or high postpulse permeability, $X_{leak} = 0.79 \pm 0.1$. Similar results for X_{leak} were obtained when evaluating the leakage of sulforhodamine (not shown). Interestingly, after temperature treatment, the occurrence frequencies of both the vesicle rupture and leaky state were significantly decreased, as shown in Fig. 2 *C* (heated agarose-GUVs). The decreased values of X_{leak} (0.3 $\pm$ 0.14) and $X_{rupture}$ (0.05 $\pm$ 0.06) after heating suggest reduction in the amount of encapsulated agarose, which partially restores the agarose-free vesicle responses. The pulse responses as reported in Fig. 2 *C* depend neither on agarose type nor on membrane composition.
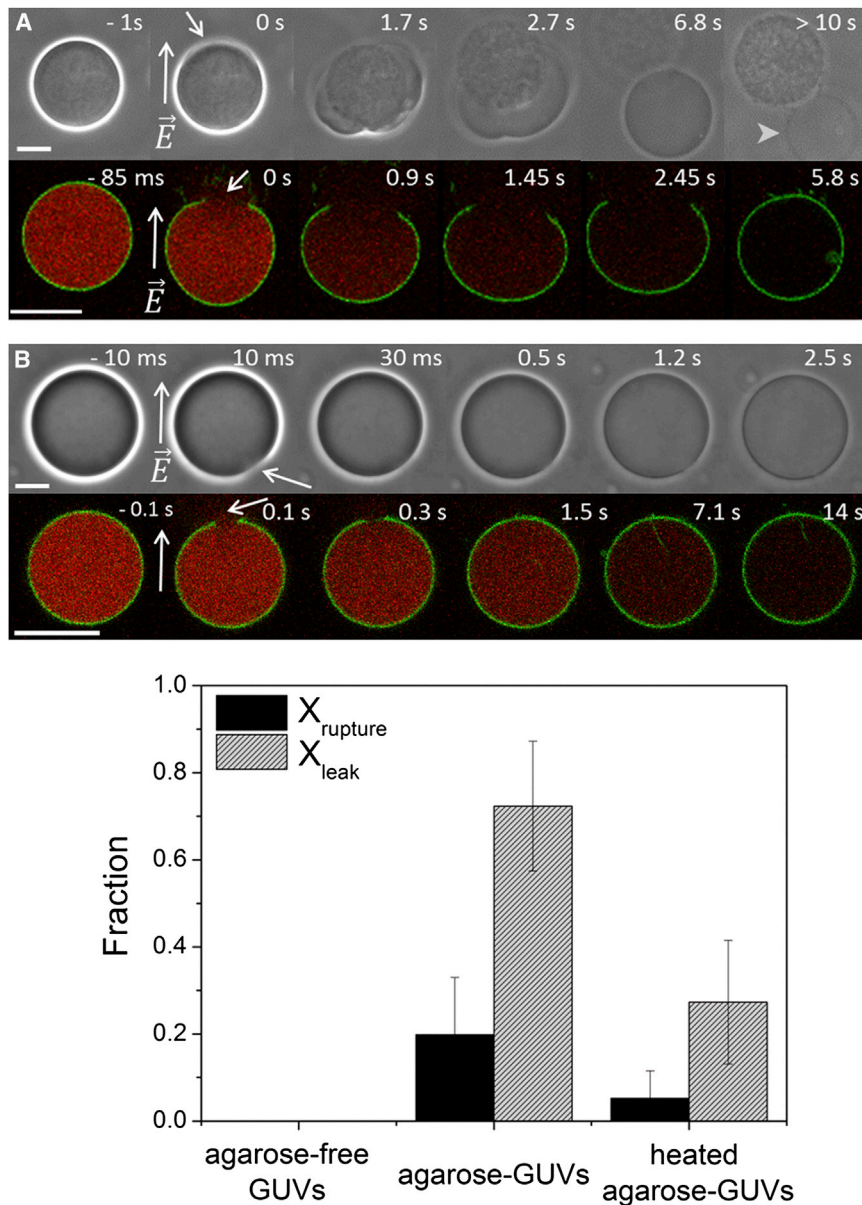
FIGURE 2 Effects of entrapped polymer on agarose-GUVs upon poration. (*A*) Vesicle rupture and expulsion of a gel-like meshwork through a macropore observed on two different vesicles. (*B*) Loss of sugar asymmetry and leakage of entrapped fluorescent dye. Upper rows: phase contrast. Lower rows: confocal microscopy. The membrane is labeled with 0.5 mol % DPPE-NBD (*green*) and the encapsulated dye is 2.5 μM sulfo-rhodamine (*red*). The times indicated on top of each snapshot are relative to the moment of pulse application (*time* 0). The field direction is indicated on the second image in the sequences. Arrows point to visible macropores. Arrowhead points to the GUV after expulsion of the meshwork and pore closure; above, one can also see the expulsed agarose meshwork. Bars: 20 μm. The complete sequences of panel *A* (*phase contrast*) and *B* (*confocal microscopy*) are shown in the Supporting Material (Movie S1 and Movie S2, respectively). (*C*) Quantification of the fraction of GUVs, which exhibit rupture with expulsion (X$_{rupture}$) or contrast loss (X$_{leak}$), for agarose-free GUVs, agarose-GUVs, and heated agarose-GUVs as observed under phase contrast. At least four different measurements, each containing 10–20 GUVs/chamber from two different batches were performed. X$_{leak}$ is calculated in respect to nonruptured vesicles, see text for details. Membrane composition: POPC/POPG 8:2. To see this figure in color, go online.

Similar results were obtained for GUVs grown in ultralow gelling temperature agarose (Fig. S4 *A*) and for neutral POPC GUVs (Fig. S4 *B*). The release of encapsulated agarose during temperature treatment also does not depend on membrane composition (Fig. S4 *C*).

The long-lived permeable state observed for most agarose-GUVs after poration can allow the passage of different entrapped material. Apart from small sugar and fluorescent molecules, which are released simultaneously (Fig. S5 *A*), agarose itself and even small vesicles can cross the bilayer, as shown in the Supporting Material (Fig. S5, *B–D*). The remaining submicron pores can even reopen into macropores in some cases. An example of that is shown in Fig. S5 *C* and Movie S3, where an agarose-GUV, which

has apparently resealed after pulse application, exhibits the opening of a macropore through which viscous agarose leaks out. Interestingly, in some cases agarose gel is left stably trapped in the pore, physically obstructing the resealing of the vesicle (see Fig. S5 *C* and Movie S3). As a consequence of defective resealing, the membrane remains highly permeable allowing exchange of material. Therefore, the origin of the permeable state appears to be the presence of agarose, which hinders membrane resealing. Vesicle rupture combined with expulsion of encapsulated gel-like meshwork represents simply an extreme case of the same phenomenon. After electroporation, only a small fraction (~15%) of the agarose-GUVs exhibits recovered membrane integrity as agarose-free GUVs do.

To better resolve the process of membrane leakage and investigate its dynamics, fast fluorescence recording at 5 ms temporal resolution was used in epifluorescence microscopy. We followed the leakage of the fluorescent dye sulforhodamine entrapped in agarose-GUVs and compared it with data acquired for agarose-free and heated agarose-GUVs; see Fig. 3. Pulse application leads to fast release of a fraction (~15%) of the encapsulated dye through the formed macropores while these pores are opened, as pointed by the arrows in Fig. 3, *A* and *B*. After this step, the fluorescence intensity remains constant for the agarose-free and heated agarose-GUVs, indicating that membrane integrity has been restored. For agarose-GUVs, however, the step is followed by slow and full release of the encapsulated dye (see the *period 1.4–7 s* in the sequence in Fig. 3 *A* and Fig. 3 *B*, *blue open circles*, 1 s after the pulse). This after-pulse increase in permeability presumably arises because of persisting submicroscopic pores or opening/widening of pores as discussed previously (see also Fig. S6). Similar two-step trends are observed from flu-
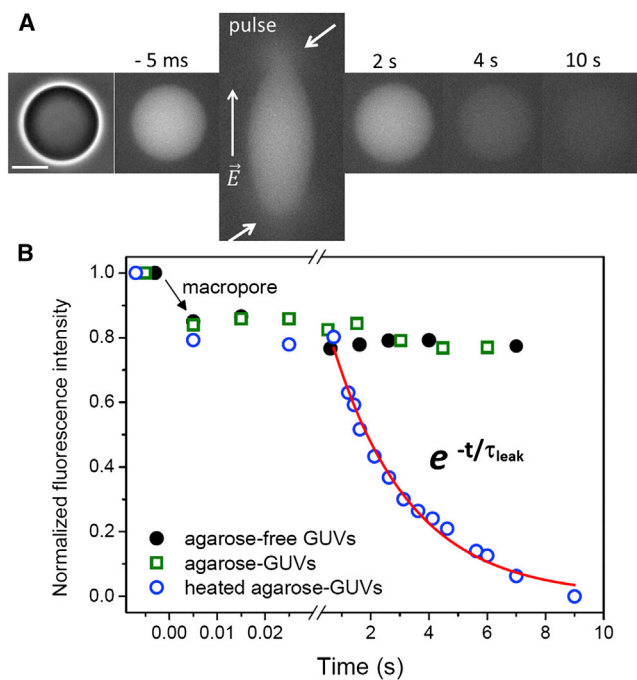

FIGURE 3 Kinetics of dye release after electroporation obtained with epifluorescence microscopy. (*A*) Sequence showing the release of sulforhodamine (initial internal concentration 2.5 μM) from an agarose-GUV after poration. The field direction is shown on the first snapshot. The time relative to pulse application ($t = 0$) is shown on each snapshot. Arrows indicate the location of the macropores observed by transient release of the dye. Bar: 20 μm. (*B*) Kinetics of dye release for the agarose-GUV shown in *A* (*blue open circles*), one typical agarose-free (*black solid circles*), and heated agarose-GUVs (*green open squares*). The red curve represents the exponential fit to the second (*slow*) leakage process, τ_{leak}. The background fluorescence was subtracted and the data were normalized by the fluorescence intensity difference before the pulse. The postpulse variation in fluorescence intensity shown for agarose-free and heated agarose-GUVs arises from small differences in the focal plane. To see this figure in color, go online.

orescently labeled agarose (not shown). Postpulse leakage follows an exponential decay with a characteristic time τ_{leak} (*red curve*). The values for τ_{leak} are very heterogeneous (19.2 ± 15.2 s), reflecting the large heterogeneity in the agarose amount encapsulated in the vesicles and the variance in pore sizes.

Previously, we showed that residual agarose encapsulated in GUVs alters membrane integrity, as seen by the presence of persisting pores leading to high and long-lived membrane permeability, and, less often, causes vesicle rupture and expulsion of an encapsulated gel-like meshwork. In the following, we address the question whether the vesicle mechanical responses to an applied DC pulse are affected by the presence of the encapsulated polymer in cases when vesicle rupture and expulsion is not observed. Mechanical responses after an applied electric pulse were monitored in terms of relaxation times of the vesicle deformation and pore closure times. Only porated vesicles with no excess area (i.e., nonfluctuating vesicles) were analyzed, in which relaxation follows a single exponential decay with characteristic time τ_{relax} (termed τ_2 previously (31)). The degree of vesicle deformation can be assessed by the ratio between the two semiaxes a and b of the prolate shape, see cartoon in Fig. 4 *B*. The pore closure time, T_{pore}, was defined as the time a pore takes until complete closure judging from the restoring of the vesicle halo in phase contrast images. Note that in this way, submicroscopic pores are not detected. In Fig. 4, *A* and *B*, we show how τ_{relax} and T_{pore} are extracted from vesicle deformation and poration. A sequence of phase contrast images of vesicle deformation for a typical agarose-GUV is given in Fig. 4 *A*. The graph below displays the aspect ratio a/b as a function of time for this particular vesicle. The data are fitted to a single exponential decay with characteristic time τ_{relax}. The time interval, in which the macropores (indicated with *arrows*) are observed, T_{pore}, is shaded in gray in Fig. 4 *B*.

Quantitative measurements of τ_{relax} and T_{pore} were done for agarose-free, agarose-, and heated agarose-GUVs and are shown in Fig. 4 *C*. The values of $\tau_{relax} = 9.8 ± 4$ ms and $T_{pore} = 52 ± 25$ ms for agarose-free GUVs are in agreement with our previous report for bare egg-PC vesicles (31). In contrast, the relaxation times of agarose-GUVs, $\tau_{relax} = 20 ± 10$ ms, are significantly longer. Moreover, the larger scatter in the data indicates large variation in the amount of entrapped agarose in the different vesicles in the population. The values of $T_{pore} = 60 ± 25$ ms obtained for GUVs grown in low gelling temperature agarose are quite similar to those observed for agarose-free GUVs. However, the measurements of T_{pore} are rather underestimated for agarose-GUVs, because T_{pore} were only measured for nonruptured vesicles (see Fig. 2 *C*). For agarose-GUVs exhibiting rupture with expulsion (see Fig. 2), T_{pore} would be in the seconds to minutes timescale. Similar results were obtained for pure POPC agarose-GUVs or GUVs made in ultralow gelling temperature agarose (Fig. S7). For the latter case,
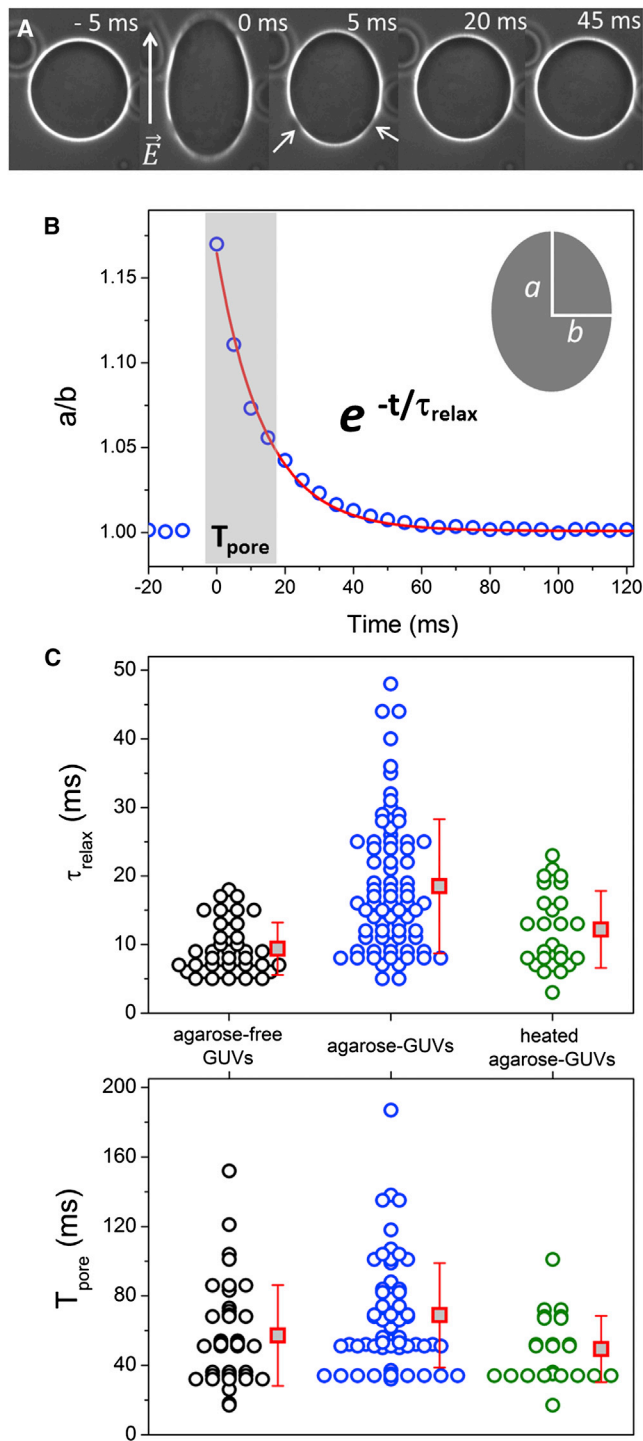
FIGURE 4 Relaxation time (τ_{relax}) and pore lifetime (T_{pore}) in porated vesicles. (A) Sequence of a typical agarose-GUV upon application of a pulse. The field direction is indicated in the first snapshot. Numbers represent time (time 0 marks the detection of the pulse as GUV response). Arrows point to macropores. Bar: 20 μm. (B) Aspect ratio a/b measured in the vesicle shown in A as a function of time. The cartoon shows the vesicle semiaxis a and b. The red curve shows the exponential fit with characteristic time τ_{relax}. The time interval with length T_{pore} when macropores are detected is shaded in gray. (C) Values of τ_{relax} and T_{pore} for agarose-free, agarose-, and heated agarose-GUVs—black, blue, and red circles, respec-

some of the vesicles display very slow pore closure times (T_{pore} up to 1 min), similar to ruptured agarose-GUVs.

The effect of temperature treatment on the mechanical response of agarose-GUVs in terms of vesicle relaxation and macropore lifetime was also investigated. After temperature treatment, both τ_{relax} (12.2 $\pm$ 5.4 ms) and T_{pore} (49.3 $\pm$ 19.1 ms) for heated agarose-GUVs displayed values similar to those obtained for agarose-free GUVs, also with low heterogeneity as shown in Fig. 4 C. This again indicates that temperature treatment at least partially recovers the mechanical behavior of agarose-free GUVs, similar to observations on the fractions X_{leak} and $X_{rupture}$ of vesicles in leaky state and exhibiting rupture.

Finally, we investigated whether hindered mechanical responses of agarose- GUVs occurred also in the absence of macroporation. For this, a weaker electric pulse (0.6 kV.cm^{-1}/600 μs) was applied to GUVs not visibly displaying a gel-like meshwork, i.e., with a smaller amount of encapsulated agarose. Such pulses below the electroporation threshold cause small prolate deformation without the formation of macropores. After the pulse, the vesicle is expected to relax to its original spherical shape with a fast relaxation time, τ_1, on the order of 0.1 ms as previously observed on agarose-free egg-PC GUVs (31). We assessed this relaxation using a fast camera at 0.1 ms temporal resolution. Fig. 5 A shows a sequence of deformation/relaxation in the absence of macroporation of an agarose-GUV, and the respective aspect ratio a/b as a function of time (Fig. 5 B). The relaxation process is well fit with a single exponential decay with characteristic time τ_1. Fig. 5 C shows the distribution of τ_1 for all systems studied. Fast relaxation times for agarose-free GUVs (τ_1 ~0.35 $\pm$ 0.09 ms) are in agreement with previous data for pure egg-PC GUVs (31). However, the values for agarose-GUVs (τ_1 ~0.59 $\pm$ 0.27) are on average almost twice higher than those obtained for agarose-free GUVs. Moreover, the values of τ_1 are very scattered for agarose-GUVs (note the standard deviation), similar to the scatter observed in τ_{relax} (see Fig. 4 C). Recently, the relaxation process was shown to predominantly depend on vesicle properties such as tension and size and fluid characteristic such as the viscosity contrast across the membrane (38). Although the former would be similar in agarose-free vesicles and in agarose-GUVs, the viscosity of agarose solutions (39) is quite different from that of sugar solutions resulting in longer relaxation times, as observed here. Furthermore, the viscoelastic nature of agarose gels has been shown to affect the shape of giant vesicles upon osmotic shrinking (40). Our observations indicate that temperature treatment, leading to a decrease in the amount of entrapped agarose, recovers the relaxation times

tively. Each point represents a measurement on a single vesicle. The values of T_{pore} have a lower limit of 17 ms corresponding to the temporal resolution of the camera. Red squares show mean values with standard deviations. To see this figure in color, go online.
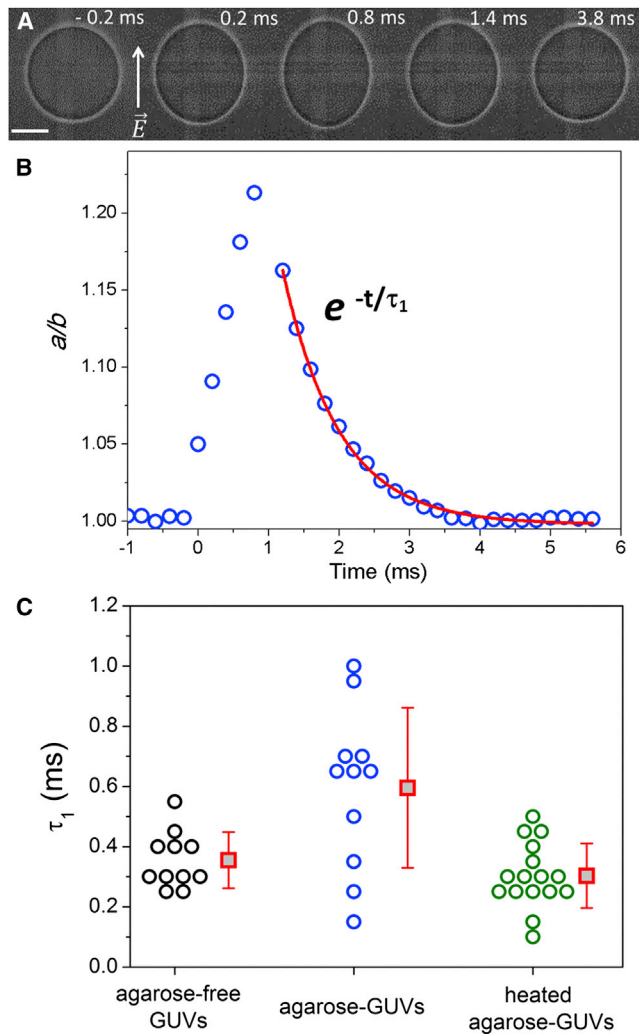
FIGURE 5 Fast relaxation times (τ_1) in the absence of macroporation. (A) Sequence of images of an agarose-GUV during and after pulse application (0.6 kV.cm^{-1}/600 μs). Numbers in the images represent time (time 0 is set as the beginning of the pulse). Bar: 10 μm. (B) Aspect ratio a/b as a function of time and subsequent relaxation data (*blue open circles*) for the vesicle shown in panel A. Red curve is the fit with a single exponential decay with characteristic time τ_1. (C) τ_1 values for agarose-free GUVs (*black*), agarose-GUVs (*blue*), and heated agarose-GUVs (*green*). Each data point represents one vesicle. Three consecutive pulses, spaced by >1 min, were applied to each vesicle and the three obtained τ_1 values were averaged for each GUV. No difference in vesicle response was observed for the three consecutive pulses applied to the same GUV (not shown). Red squares are average values with standard deviation. To see this figure in color, go online.

of the vesicles to values ($\tau_1 \sim 0.3 \pm 0.1$ ms, see Fig. 5 C) similar to those obtained for agarose-free GUVs.

DISCUSSION

In this work, we show that GUVs produced by spontaneous swelling of hybrid films of agarose and lipids contain an encapsulated residual amount of agarose, which, in turn, significantly changes the vesicle mechanics. We expect

that the mechanical properties of vesicles grown at high ionic strength (not measured here because of the method limitations) will be altered even more significantly considering the enhanced adsorption of the polymer to the membrane in this case (see Fig. S1 B). In salt-free conditions, the polymer is entrapped in the GUV lumen with no indication of binding to the membrane and change of lipid lateral diffusion (Fig. S2). The degree of polymer encapsulation varies significantly when comparing vesicles from the same batch (Fig. 1). As a result, the response of the vesicles to an applied electric pulse exhibits large heterogeneity (Figs. 2 and 3). For the vesicles in which gel-like meshwork is formed, favored by high polymer concentration, rupture associated with expulsion of the meshwork is observed. For most of the remaining nonruptured GUVs (and probably also for the resealed ruptured vesicles), persisting submicron pores lead to material exchange and increased membrane permeability. The hindered mechanical responses were observed even in the absence of membrane poration (upon application of weak pulses), as demonstrated by the slower relaxation of the deformed vesicles (Fig. 5). For all properties studied here, heating of the GUVs above the melting temperature of agarose at least partially recovered the mechanical response of the vesicles, because it allowed the release of a large amount of the encapsulated agarose.

A couple of plausible mechanisms could drive the release of polymer and sugars upon heating of the agarose-GUVs. On the one hand, membrane pore-like defects, which are expected to occur and develop more frequently at higher temperature, could become stabilized by agarose molecules in a similar way in which the lifetime of pores induced by electroporation is increased. In fact, even at room temperature, few agarose-GUVs were found to have lost the original sugar contrast. Therefore, agarose can be trapped in such pore-like defects even in the absence of electroporation, but the release and permeation are certainly enhanced either by increase in temperature or pulse application. On the other hand, upon heating, the polymer gel could be effectively expanding in volume and agarose aggregates could be disrupted. This would increase the internal (osmotic) pressure leading to vesicle rupture and loss of contrast.

As hinted previously, the origin of the high membrane permeability of agarose-GUVs following the application of electroporating pulses (or heating) can be explained by the presence of agarose polymers entrapped to a different extent across the membrane pores, thus preventing normal membrane resealing driven by membrane edge tension. Apart from physically obstructing pore closure, agarose polymers may get intercalated between the lipid headgroups in the pore region thus lowering the edge tension of the membrane. The latter would be consistent with recent findings on the adsorption of sugars on membranes (41). Sugars were also found to modulate the membrane bending rigidity (for a review see (5)). Fluctuation analysis performed following the protocol in (35) suggested no effect of

encapsulated agarose on membrane bending rigidity (Fig. S8), as speculated in an earlier study (23). However, the method requires the use of fluctuating vesicles, and therefore only vesicles with low concentration of encapsulated agarose were selected.

The vesicle responses to electrodeformation and poration are summarized in Fig. 6 for agarose-free and agarose-GUVs with different concentrations of encapsulated agarose. Weaker pulses (*orange arrows*) lead to deformation
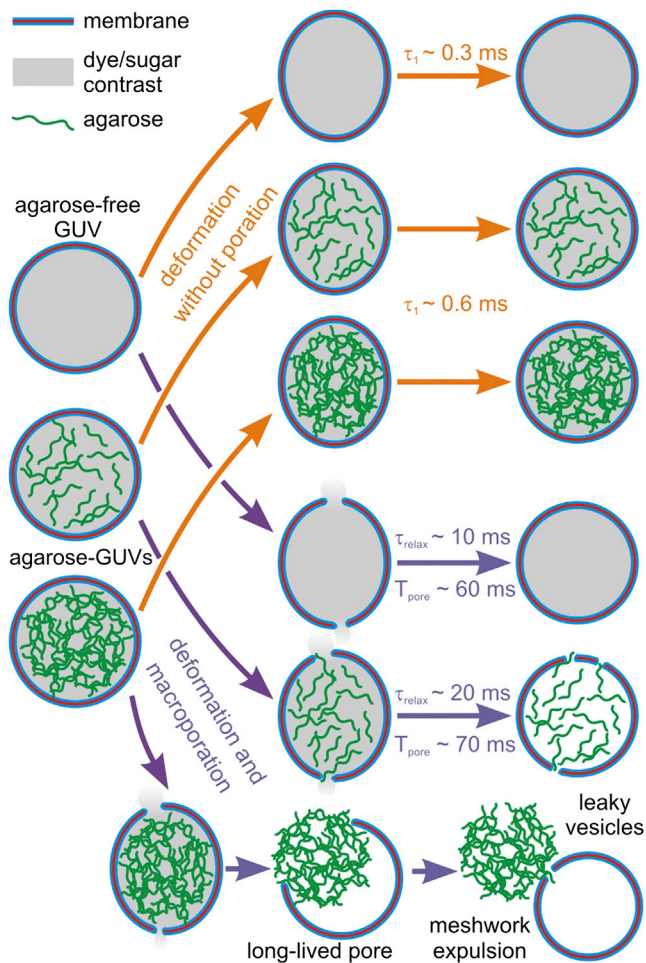

FIGURE 6 Sketch of all possible scenarios for the response of agarose-free and agarose-GUVs exposed to electrodeformation and poration. Sulforhodamine and sucrose (represented as *gray shading inside the vesicles*) and agarose (*green*) are initially encapsulated inside the agarose-rich vesicles. Upon pulse application, the vesicles deform and may porate depending on pulse strength. The vesicle relaxation times in the presence and absence of poration (τ_{relax} and τ_1, respectively) are longer for agarose-GUVs. When exposed to pulses causing macroporation, the agarose-free vesicles porate and fully reseal. For most vesicles (containing low and intermediate concentration of encapsulated agarose as exemplified in the cartoon by the vesicles filled with less agarose), after closure of the macropores with characteristic lifetime T_{pore}, a leaky state is maintained resulting from the presence of agarose in the formed pores. Vesicles with high agarose concentration expulse a gel-like meshwork through the formed macropore, accompanied with fast and total mixing of internal and external contents. To see this figure in color, go online.

without macroporation, whereas strong pulses (*purple arrows*) lead to macroporation, after which most agarose-GUVs reseal retaining the sugar/dye contrast. In the case of agarose-GUVs with high concentration of encapsulated agarose, the gel meshwork is expulsed through a large membrane pore (with diameter of the order of the vesicle size) and the vesicle recloses with lost contrast. For the agarose-GUVs, the relaxation of deformed vesicles (without and with poration) is slowed down as compared to that of agarose-free GUVs. After the pulse, agarose-GUVs exhibit pore(s), which can be stable or numerous enough to allow exchange of materials across the membrane. The reported vesicle response was obtained for agarose-GUVs in salt-free media. Unfortunately, our method based on vesicle deformation under DC pulses cannot be easily applied to probe the mechanical response of GUVs in physiological salt conditions. However, similar or even a more pronounced effect on the vesicle mechanics is to be expected, because agarose is found encapsulated in the lumen as well as enriched at the membrane of vesicles grown in this condition (see Fig. S1 *B*).

We will now dwell on the implications of our findings on the use of agarose-GUVs. Surely, the preparation method based on hybrid films of agarose and lipids is simple and straightforward and allows production of GUVs of virtually any composition, even in the presence of salt, conditions not met by the classical and widely used electroformation method. However, this study emphasizes that one must be aware of possible artifactual behavior of agarose-GUVs. In particular, special caution should be applied when the studied system involves overall morphological changes in the vesicle or any kind of mechanical response of the membrane such as bending, but also pore formation. Our conclusion is that agarose vesicles should not be employed for instance when extracting membrane properties from vesicle deformation (4,35), pore formation by membrane active molecules (8,42,43), protein-induced membrane curvature (44–46), initial steps in membrane solubilization by detergents (47,48), and vesicle reshaping during changes in the phase state of the bilayer (7,49). On the other hand, studies focusing on membrane properties such as lateral mobility of membrane components and phase separation, or membrane protein reconstitution might still profit from the use of agarose-GUVs.

Some possible ways can be envisioned to still employ vesicles formed from hybrid films of polymer and lipids without the contamination of the remaining polymer. Here, we showed that temperature treatment of agarose-GUVs leads to a significant reduction in the amount of encapsulated agarose, mostly restoring the bare vesicle responses. This approach, however, can also change the membrane properties in other ways, especially for those made of high melting temperature lipids, leading for instance to changes in membrane permeability upon crossing the lipid phase transition. Moreover, lipid oxidation might be favored

at higher temperatures. Another approach for preparing vesicles from hybrid films is to use alternative polymers. In their work, Horger et al. (22) suggest that films of cross-linked polyacrylamide gels could be used instead of agarose gels. Very recently, Weinberger et al. (29) have replaced agarose for PVA, a less water-soluble polymer, to produce GUVs. It was shown by fluorescence imaging that there is no indication of residual polymer, either encapsulated or bound to the membranes (fluorescence imaging does not fully exclude the possibility of remaining polymers present at the membrane and in the vesicles). Possible side effects on the mechanical properties have not been described. However, in contrast to agarose, PVA cannot be used at relatively high temperatures (over 50°C) due to loss of the gel integrity. Furthermore, difficulties with desorbing these vesicles from the polymer cushion exist. Another more recent work (50) reported a high yield of polymer-free GUVs grown on a covalently cross-linked hydrogel substrate, with the advantage of controlling vesicle size distribution through the cross-link density. These new protocols present a great improvement on the method and show that the use of alternative polymers can potentially circumvent hindering effects of remaining polymer on GUVs.

Here, we have proposed a comprehensive set of approaches that can be of future help to evaluate the degree to which residual molecules in general can influence the membrane behavior.

SUPPORTING MATERIAL

Eight figures and three movies are available at http://www.biophysj.org/biophysj/supplemental/S0006-3495(14)00852-2.

REFERENCES

1. Menger, F. M., and J. S. Keiper. 1998. Chemistry and physics of giant vesicles as biomembrane models. *Curr. Opin. Chem. Biol.* 2:726–732.

2. Dimova, R., S. Aranda, …, R. Lipowsky. 2006. A practical guide to giant vesicles. Probing the membrane nanoregime via optical microscopy. *J. Phys. Condens. Matter.* 18:S1151–S1176.

3. Fenz, S. F., and K. Sengupta. 2012. Giant vesicles as cell models. *Integr. Biol. (Camb).* 4:982–995.

4. Evans, E., and W. Rawicz. 1990. Entropy-driven tension and bending elasticity in condensed-fluid membranes. *Phys. Rev. Lett.* 64:2094–2097.

5. Dimova, R. 2014. Recent developments in the field of bending rigidity measurements on membranes. *Adv. Colloid Interface Sci.* 208:225–234.

6. Lipowsky, R., and R. Dimova. 2003. Domains in membranes and vesicles. *J. Phys. Condens. Matter.* 15:S31–S45.

7. Baumgart, T., S. T. Hess, and W. W. Webb. 2003. Imaging coexisting fluid domains in biomembrane models coupling curvature and line tension. *Nature.* 425:821–824.

8. Tamba, Y., and M. Yamazaki. 2005. Single giant unilamellar vesicle method reveals effect of antimicrobial peptide magainin 2 on membrane permeability. *Biochemistry.* 44:15823–15833.

9. Laurencin, M., T. Georgelin, …, C. Ménager. 2010. Interactions between giant unilamellar vesicles and charged core-shell magnetic nanoparticles. *Langmuir.* 26:16025–16030.

10. Lira, R. B., M. A. B. L. Seabra, …, A. Fontes. 2013. Studies on intracellular delivery of carboxyl-coated CdTe quantum dots mediated by fusogenic liposomes. *J. Mater. Chem. B.* 1:4297–4305.

11. Li, Y., R. Lipowsky, and R. Dimova. 2008. Transition from complete to partial wetting within membrane compartments. *J. Am. Chem. Soc.* 130:12252–12253.

12. Chiu, D. T., C. F. Wilson, …, R. N. Zare. 1999. Chemical transformations in individual ultrasmall biomimetic containers. *Science.* 283:1892–1895.

13. Yang, P., R. Lipowsky, and R. Dimova. 2009. Nanoparticle formation in giant vesicles: synthesis in biomimetic compartments. *Small.* 5:2033–2037.

14. Noireaux, V., and A. Libchaber. 2004. A vesicle bioreactor as a step toward an artificial cell assembly. *Proc. Natl. Acad. Sci. USA.* 101:17669–17674.

15. Walde, P., K. Cosentino, …, P. Stano. 2010. Giant vesicles: preparations and applications. *ChemBioChem.* 11:848–865.

16. Dimova, R. 2012. Giant vesicles: a biomimetic tool for membrane characterization. *In* Advances in Planar Lipid Bilayers and Liposomes. Aleš Iglič, editor.. Academic Press, NY, pp. 1–50.

17. Angelova, M. I., and D. S. Dimitrov. 1986. Liposome electroformation. *Faraday Discuss.* 81:303–311.

18. Pott, T., H. Bouvrais, and P. Méléard. 2008. Giant unilamellar vesicle formation under physiologically relevant conditions. *Chem. Phys. Lipids.* 154:115–119.

19. Akashi, K., H. Miyata, …, K. Kinosita, Jr. 1996. Preparation of giant liposomes in physiological conditions and their characterization under an optical microscope. *Biophys. J.* 71:3242–3250.

20. Moscho, A., O. Orwar, …, R. N. Zare. 1996. Rapid preparation of giant unilamellar vesicles. *Proc. Natl. Acad. Sci. USA.* 93:11443–11447.

21. Richmond, D. L., E. M. Schmid, …, D. A. Fletcher. 2011. Forming giant vesicles with controlled membrane composition, asymmetry, and contents. *Proc. Natl. Acad. Sci. USA.* 108:9431–9436.

22. Horger, K. S., D. J. Estes, …, M. Mayer. 2009. Films of agarose enable rapid formation of giant liposomes in solutions of physiologic ionic strength. *J. Am. Chem. Soc.* 131:1810–1819.

23. Tsai, F. C., B. Stuhrmann, and G. H. Koenderink. 2011. Encapsulation of active cytoskeletal protein networks in cell-sized liposomes. *Langmuir.* 27:10061–10071.

24. Ikenouchi, J., M. Suzuki, …, M. Umeda. 2012. Lipid polarity is maintained in absence of tight junctions. *J. Biol. Chem.* 287:9525–9533.

25. Drücker, P., M. Pejic, …, V. Gerke. 2013. Lipid segregation and membrane budding induced by the peripheral membrane binding protein annexin A2. *J. Biol. Chem.* 288:24764–24776.

26. Hansen, J. S., J. R. Thompson, …, N. Malmstadt. 2013. Lipid directed intrinsic membrane protein segregation. *J. Am. Chem. Soc.* 135:17294–17297.

27. Katayama, S., I. Nakase, …, S. Futaki. 2013. Effects of pyrenebutyrate on the translocation of arginine-rich cell-penetrating peptides through artificial membranes: recruiting peptides to the membranes, dissipating liquid-ordered phases, and inducing curvature. *Biochim. Biophys. Acta.* 1828:2134–2142.

28. Saliba, A. E., I. Vonkova, …, A. C. Gavin. 2014. A quantitative liposome microarray to systematically characterize protein-lipid interactions. *Nat. Methods.* 11:47–50.

29. Weinberger, A., F. C. Tsai, …, C. Marques. 2013. Gel-assisted formation of giant unilamellar vesicles. *Biophys. J.* 105:154–164.

30. Needham, D., and R. M. Hochmuth. 1989. Electro-mechanical perme-abilization of lipid vesicles. Role of membrane tension and compress-ibility. *Biophys. J.* 55:1001–1009.

31. Riske, K. A., and R. Dimova. 2005. Electro-deformation and poration of giant vesicles viewed with high temporal resolution. *Biophys. J.* 88:1143–1155.

32. Riske, K. A., and R. Dimova. 2006. Electric pulses induce cylindrical deformations on giant vesicles in salt solutions. *Biophys. J.* 91:1778–1786.

33. Riske, K. A., R. L. Knorr, and R. Dimova. 2009. Bursting of charged multicomponent vesicles subjected to electric pulses. *Soft Matter.* 5:1983–1986.

34. Portet, T., and R. Dimova. 2010. A new method for measuring edge ten-sions and stability of lipid bilayers: effect of membrane composition. *Biophys. J.* 99:3264–3273.

35. Gracià, R. S., N. Bezlyepkina, …, R. Dimova. 2010. Effect of choles-terol on the rigidity of saturated and unsaturated membranes: fluctua-tion and electrodeformation analysis of giant vesicles. *Soft Matter.* 6:1472–1482.

36. Bezlyepkina, N., R. S. Gracià, …, R. Dimova. 2013. Phase diagram and tie-line determination for the ternary mixture DOPC/eSM/cholesterol. *Biophys. J.* 104:1456–1464.

37. Normand, V., D. L. Lootens, …, P. Aymard. 2000. New insight into agarose gel mechanical properties. *Biomacromolecules.* 1:730–738.

38. Zhang, J., J. D. Zahn, …, H. Lin. 2013. A transient solution for vesicle electrodeformation and relaxation. *Phys. Fluids.* 25:071903.

39. Fernandez, E., D. Lopez, …, K. Dusek. 2008. Rheological and thermal properties of agarose aqueous solutions and hydrogels. *J. Polym. Sci. Part B: Pol. Phys.* 46:322–328.

40. Viallat, A., J. Dalous, and M. Abkarian. 2004. Giant lipid vesicles filled with a gel: shape instability induced by osmotic shrinkage. *Biophys. J.* 86:2179–2187.

41. Andersen, H. D., C. Wang, …, P. Westh. 2011. Reconciliation of opposing views on membrane-sugar interactions. *Proc. Natl. Acad. Sci. USA.* 108:1874–1878.

42. Domingues, T. M., K. A. Riske, and A. Miranda. 2010. Revealing the lytic mechanism of the antimicrobial peptide gomesin by observing giant unilamellar vesicles. *Langmuir.* 26:11077–11084.

43. Islam, M. Z., H. Ariyama, …, M. Yamazaki. 2014. Entry of cell-pene-trating peptide transportan 10 into a single vesicle by translocating across lipid membrane and its induced pores. *Biochemistry.* 53:386–396.

44. Stachowiak, J. C., E. M. Schmid, …, C. C. Hayden. 2012. Membrane bending by protein-protein crowding. *Nat. Cell Biol.* 14:944–949.

45. Roux, A., G. Koster, …, P. Bassereau. 2010. Membrane curvature con-trols dynamin polymerization. *Proc. Natl. Acad. Sci. USA.* 107:4141–4146.

46. Bacia, K., E. Futai, …, R. Schekman. 2011. Multibudded tubules formed by COPII on artificial liposomes. *Sci. Rep.* 1:17.

47. Nomura, F., M. Nagata, …, K. Takiguchi. 2001. Capabilities of lipo-somes for topological transformation. *Proc. Natl. Acad. Sci. USA.* 98:2340–2345.

48. Sudbrack, T. P., N. L. Archilha, …, K. A. Riske. 2011. Observing the solubilization of lipid bilayers by detergents with optical microscopy of GUVs. *J. Phys. Chem. B.* 115:269–277.

49. Riske, K. A., L. Q. Amaral, and M. T. Lamy. 2009. Extensive bilayer perforation coupled with the phase transition region of an anionic phos-pholipid. *Langmuir.* 25:10083–10091.

50. López Mora, N., J. S. Hansen, …, A. Kros. 2014. Preparation of size tunable giant vesicles from cross-linked dextran(ethylene glycol) hydrogels. *Chem. Commun. (Camb.).* 50:1953–1955.